IS THERE A COMMON ALPHA-EFFICIENCY IN POLYMINERAL SAMPLES MEASURED BY VARIOUS INFRARED STIMULATED LUMINESCENCE PROTOCOLS?

CHRISTOPH SCHMIDT[1], JANINA BÖSKEN[2, 3] and THOMAS KOLB[1]

[1]*Chair of Geomorphology & BayCEER, University of Bayreuth, 95440 Bayreuth, Germany*
[2]*Department of Geography, RWTH Aachen University, Templergraben 55, 52056 Aachen, Germany*
[3]*Institute of Geography, University of Cologne, Albertus-Magnus-Platz, 50923 Cologne, Germany*

Abstract: Dating of polymineral silt-sized samples by use of post-infrared infrared stimulated luminescence (pIRIR) protocols at elevated temperature has recently gained attraction due to assumed lower rates of anomalous fading. The α-efficiency (or a-value) associated with the pIRIR signals as an integral part of age calculation has, however, not yet been sufficiently constrained. Here we present a set of 65 a-values determined for 47 samples collected across Europe with two different IRSL protocols in two laboratories. By testing the basic preconditions for application of the single-aliquot regeneration (SAR) procedure to constrain a-values and by comparing SAR results to a-values obtained by multiple-aliquot protocols, we demonstrate that SAR-derived a-values are reliable for the majority of samples. While aliquot size and signal resetting mode prior to α-regeneration do not appear to affect the resulting a-value, we detected significant differences in mean a-values measured in the two laboratories. For the pIRIR$_{290}$ signal, a-values average to 0.085 ± 0.010 (Bayreuth) and 0.101 ± 0.014 (Cologne), while a modified SAR protocol yields 0.081 ± 0.008 (Bayreuth). Whereas provenance-specific differences in a-values might be masked by overall scatter, systematic offsets between laboratories are attributed to technical issues such as heater and source calibration. Based on the present data set, use of the same routine dating equipment is strongly advised for both dose and a-value measurements.

Keywords: luminescence, infrared stimulated luminescence – IRSL, polymineral samples, alpha-efficiency, a-value, loess.

1. INTRODUCTION

Measuring the infrared stimulated luminescence (IRSL) of K-feldspar or polymineral separates at elevated temperatures (>150°C) after initial IRSL stimulation at 50°C (IRSL$_{50}$) has gained considerable popularity for estimating the equivalent dose (D_e) in retrospective do-simetry (e.g., Thomsen *et al.*, 2008; Thiel *et al.*, 2011; Reimann and Tsukamoto, 2012). This technique – usually referred to as post-IR IRSL or pIRIR – offers access to feldspar-derived luminescence signals less affected by so-called anomalous fading (Wintle, 1973). The conceptual model explaining these lower fading rates builds upon an increased distance between trapping and recombination sites as stimulation temperature is raised, resulting in a decreased probability of tunneling recombination of opposite charge carriers (e.g., Jain and Ankjærgaard, 2011; Buylaert *et al.*, 2012). There is however a trade-off between low fading rates of pIRIR signals and signal

Corresponding author: C. Schmidt
e-mail: christoph.schmidt@uni-bayreuth.de

bleachability, *i.e.*, the pIRIR stimulation temperature is inversely related to the optical resetting rate of the respective signal, while part of the signal remains unaffected by sunlight exposure (Li and Li, 2011). This unbleachable residual has occasionally been determined in the laboratory by applying some sort of residual subtraction method in order to isolate the optically sensitive component from the bulk signal (e.g., Schatz *et al.*, 2012; Li *et al.*, 2013).

Commonly, either sand-sized (~90–250 μm) K-feldspar or silt-sized (~4–11 μm) polymineral grains are prepared for pIRIR measurements. While it is debatable whether the coarse grain size fraction should be HF-etched to remove the outer layer influenced by external α-radiation (e.g., Duller, 1992; Li and Li, 2011; Trauerstein *et al.*, 2014; Kenzler *et al.*, 2015), the α-dose rate has to be fully considered for fine grains (~4–11 μm). To account for the different efficiency in producing luminescence of heavy particles such as α-particles and slightly ionising radiation such as β- and γ-radiation, the so-called α-efficiency must be incorporated when calculating the dose rate (Aitken, 1985a). Among the different systems presented for quantifying α-efficiency (see Aitken, 1985b, for a summary), the *a*-value system has most widely been used both for quartz and feldspar. This system is based on the findings of Aitken and Bowman (1975) indicating that the induced luminescence per unit of generated α-track length (in $\mu m \, \mu m^{-3} = \mu m^{-2}$) is nearly independent from the α-particle's energy. Hence, the luminescence recorded after generating a certain cumulative length of α-tracks is compared with the luminescence resulting from a known β-dose to calculate the *a*-value. In the case of quartz and mono-energetic 3.7 MeV α-particles (as delivered by many ^{214}Am sources), the *a*-value is by definition equal to the *k*-value, where the ratio of luminescence induced by an α-dose (in Gy) to that induced by a β-dose (in Gy) is calculated. For non-quartz materials, a correction factor *r* relates the material-specific *a*-value to the quartz *a*-value (Aitken, 1985b). This correction factor largely depends on the density of the used material. Since the density of feldspar, however, only deviates 2% from the density of quartz, we used uncorrected *a*-values in this study.

Compared to the vast body of literature published during the past years on the application of the pIRIR protocol to various sedimentary archives, only relatively few studies determined the *a*-value individually for the samples investigated. Many authors refer to Rees-Jones (1995) when using an *a*-value of 0.08 ± 0.02, although this value is based on three samples only and – more importantly – determined for the IRSL signal recorded using a multiple-aliquot protocol and under strongly varying preheat and measurement conditions than the ones used in the respective studies (e.g., Stevens *et al.*, 2011; Thiel *et al.*, 2011; Buylaert *et al.*, 2012; Vasiliniuc *et al.*, 2012; Schmidt *et al.*, 2014). Only Biswas *et al.* (2013) reported measured pIRIR$_{290}$ *a*-values ranging from 0.036 ± 0.003 to 0.055 ± 0.002 for volcanic ash samples,

determined by administering a known α-dose to a bleached sample and recovering the equivalent β-dose using a single-aliquot regenerative dose protocol. These values are on average higher than the IRSL$_{50}$ *a*-values of these samples by a factor of 1.28 ± 0.03 (Biswas *et al.*, 2013). Successful dose recovery using either solely α-regeneration or solely β-regeneration always combined with a fixed β-test dose for normalisation led the authors to conclude that this approach of *a*-value determination is accurate. In a more comprehensive study, Kreutzer *et al.* (2014) determined pIRIR$_{225}$ *a*-values for five loess samples (polymineral fine grains) from Saxony (Germany), revealing a systematic difference between IRSL$_{50}$ and pIRIR$_{225}$ *a*-values. Furthermore, the mode of signal resetting (heating vs. bleaching) prior to α-irradiation appears to affect the size of the *a*-value (Kreutzer *et al.*, 2014). Considering the results obtained in the referenced studies above, one might suspect that the pIRIR *a*-value of polymineral fine grains correlates positively with the pIRIR stimulation temperature. It therefore appears timely to further investigate the *a*-value of the pIRIR$_{290}$ signal for a range of different samples. Specifically, the present study aims at:

1) identifying a suitable method to accurately determine pIRIR *a*-values,
2) investigating whether there is a common pIRIR$_{290}$ *a*-value, independent of sample mineralogy or provenance, and
3) clarifying whether the pIRIR$_{290}$ *a*-value is different from the pIRIR$_{225}$ *a*-value.

Many samples in our laboratories were recently measured with a distinct IRSL protocol (following the approach described in detail in Faust *et al.*, 2015) which includes a high-temperature preheat and a 20 min pause prior to IRSL measurement, in order to minimise anomalous fading. In addition to pIRIR$_{290}$ *a*-values, we therefore also report on the *a*-values determined with this procedure (termed IRSL$_F$ henceforth) in order to assess the variability of the *a*-value as a function of the IRSL/pIRIR measurement protocol. Details on both protocols employed in this study are given below.

2. SAMPLES AND SAMPLE PREPARATION

To evaluate both the variability of the pIRIR$_{290}$ *a*-value between samples of different mineralogy and geographical origin and within a set of samples originating from the same outcrop, we studied a total of 47 polymineral fine grain samples from 10 different locations in Europe. **Table 1** provides a summary of these samples.

Prior to measurement, samples were dry or wet sieved to grain sizes <63 μm, soaked in 10% HCl and 10% H_2O_2 to dissolve carbonates and oxidise organic matter, respectively, treated with 0.01 N sodium oxalate to disperse aggregates (only Cologne laboratory) and subsequently settled in a water column for distinct periods to extract the target grain size range of ~4–11 μm (application of

Table 1. *Summary of investigated samples. Sample codes BT… refer to the luminescence laboratory in Bayreuth, codes C-L… to the laboratory in Cologne; pIRIR$_{290}$ = post-IR IRSL protocol with 290°C stimulation temperature (following Thiel et al., 2011); IRSL$_F$ = IRSL protocol according to Faust et al. (2015); MAAD = multiple-aliquot additive-dose protocol applied both to the pIRIR$_{290}$ and the IRSL$_F$ emission (see main text for further details).*

Sample code	Provenance	Coordinates	Depositional environment	Applied protocols	Reference
BT1257	Titel, Serbia	45°17'42"N, 20°11'22"E	Loess	pIRIR$_{290}$	–
BT1258	Titel, Serbia	45°17'42"N, 20°11'22"E	Loess	pIRIR$_{290}$	–
BT1259	Titel, Serbia	45°17'42"N, 20°11'22"E	Loess	pIRIR$_{290}$	–
BT1337	Encantado I, Fuerteventura	28°38'20"N, 13°58'37"W	Aeolian deposits	IRSL$_F$	–
BT1339	Encantado I, Fuerteventura	28°38'18"N, 13°58'40"W	Aeolian deposits	IRSL$_F$	–
BT1340	Melian, Fuerteventura	28°40'18"N, 13°57'08"W	Aeolian deposits	IRSL$_F$	Roettig *et al.* (2017)
BT1341	Melian, Fuerteventura	28°40'18"N, 13°57'08"W	Aeolian deposits	IRSL$_F$	Roettig *et al.* (2017)
BT1342	Melian, Fuerteventura	28°40'09"N, 13°57'14"W	Aeolian deposits	IRSL$_F$	Roettig *et al.* (2017)
BT1343	Melian, Fuerteventura	28°40'09"N, 13°57'14"W	Aeolian deposits	IRSL$_F$	Roettig *et al.* (2017)
BT1344	Melian, Fuerteventura	28°40'22"N, 13°57'12"W	Aeolian deposits	MAAD (pIRIR$_{290}$, IRSL$_F$)	Roettig *et al.* (2017)
BT1345	Melian, Fuerteventura	28°40'22"N, 13°57'12"W	Aeolian deposits	MAAD (pIRIR$_{290}$, IRSL$_F$)	Roettig *et al.* (2017)
BT1421	Encantado III, Fuerteventura	28°38'21"N, 13°58'44"W	Aeolian deposits	IRSL$_F$	Roettig *et al.* (2017)
BT1423	Encantado III, Fuerteventura	28°38'21"N, 13°58'44"W	Aeolian deposits	IRSL$_F$	Roettig *et al.* (2017)
BT1424	Encantado III, Fuerteventura	28°38'21"N, 13°58'44"W	Aeolian deposits	IRSL$_F$	Roettig *et al.* (2017)
BT1425	Encantado III, Fuerteventura	28°38'21"N, 13°58'44"W	Aeolian deposits	IRSL$_F$	Roettig *et al.* (2017)
BT1426	Encantado III, Fuerteventura	28°38'21"N, 13°58'44"W	Aeolian deposits	IRSL$_F$	Roettig *et al.* (2017)
BT1432	Enamorados, Fuerteventura	28°38'05"N, 13°59'06"W	Aeolian deposits	IRSL$_F$	–
BT1513	Jable 1, Fuerteventura	28°38'38"N, 13°58'28"W	Aeolian deposits	pIRIR$_{290}$, IRSL$_F$	–
BT1514	Jable 1, Fuerteventura	28°38'38"N, 13°58'28"W	Aeolian deposits	IRSL$_F$	Roettig *et al.* (2017)
BT1515	Jable 1, Fuerteventura	28°38'38"N, 13°58'28"W	Aeolian deposits	pIRIR$_{290}$, IRSL$_F$	Roettig *et al.* (2017)
BT1517	Jable 1, Fuerteventura	28°38'38"N, 13°58'28"W	Aeolian deposits	pIRIR$_{290}$, IRSL$_F$	–
BT1519	Fuerteventura, Spain	28°39'09"N, 13°57'27"W	Aeolian deposits	pIRIR$_{290}$, IRSL$_F$	–
BT1525	Jable 2, Fuerteventura	28°38'50"N, 13°58'38"W	Aeolian deposits	pIRIR$_{290}$, IRSL$_F$	Roettig *et al.* (2017)
BT1528	Jable 2, Fuerteventura	28°38'50"N, 13°58'38"W	Aeolian deposits	pIRIR$_{290}$, IRSL$_F$	–
BT1529	Montana Roja, Fuerteventura	28°38'59"N, 13°51'08"W	Aeolian deposits	IRSL$_F$	–
BT1401	Eifel, Germany	50°04'39"N, 07°01'43"E	Quartzitic slate	pIRIR$_{290}$	Schmidt *et al.* (2017)
BT1415	Vârghis, Romania	46°12'58"N, 25°32'36"E	Aeolian cave deposit	pIRIR$_{290}$	Veres *et al.* (2018)
BT1416	Vârghis, Romania	46°12'58"N, 25°32'36"E	Aeolian cave deposit	pIRIR$_{290}$	Veres *et al.* (2018)
BT1417	Întorsura Buzăului, Romania	45°43'02"N, 26°04'13"E	Loamy hillslope deposit	pIRIR$_{290}$	–
C-L3704	Urluia, Romania	44°05'42"N, 27°54'07"E	Loess	pIRIR$_{290}$	–
C-L3707	Urluia, Romania	44°05'42"N, 27°54'07"E	Loess	pIRIR$_{290}$	Obreht *et al.* (2017)
C-L3778	Stalać, Serbia	43°40'39"N, 21°25'04"E	Loess	pIRIR$_{290}$	Bösken *et al.* (2017)
C-L3780	Stalać, Serbia	43°40'39"N, 21°25'04"E	Loess	pIRIR$_{290}$	Bösken *et al.* (2017)
C-L3784	Stalać, Serbia	43°40'39"N, 21°25'04"E	Loess	pIRIR$_{290}$	Bösken *et al.* (2017)
C-L3786	Stalać, Serbia	43°40'39"N, 21°25'04"E	Loess	pIRIR$_{290}$	Bösken *et al.* (2017)
C-L3787	Stalać, Serbia	43°40'39"N, 21°25'04"E	Pedogenetically overprinted loess	pIRIR$_{290}$	Bösken *et al.* (2017)
C-L3788	Stalać, Serbia	43°40'39"N, 21°25'04"E	Loess	pIRIR$_{290}$	Bösken *et al.* (2017)
C-L4029	Vrsac, Serbia	45°09'10"N, 21°09'30"E	Lacustrine sediment	pIRIR$_{290}$	Zeeden *et al.* (in prep.)
C-L4030	Vrsac, Serbia	45°09'10"N, 21°09'30"E	Lacustrine sediment	pIRIR$_{290}$	Zeeden *et al.* (in prep.)
C-L4031	Vrsac, Serbia	45°09'10"N, 21°09'30"E	Lacustrine sediment	pIRIR$_{290}$	Zeeden *et al.* (in prep.)
C-L3789	Ságvár, Hungary	46°49'18"N, 18°05'23"E	Loess	pIRIR$_{290}$	Bösken *et al.* (in press, a)
C-L3791	Ságvár, Hungary	46°49'18"N, 18°05'23"E	Loess	pIRIR$_{290}$	Bösken *et al.* (in press, a)
C-L3792	Ságvár, Hungary	46°49'18"N, 18°05'23"E	Loess	pIRIR$_{290}$	Bösken *et al.* (in press, a)
C-L3793	Ságvár, Hungary	46°49'18"N, 18°05'23"E	Loess	pIRIR$_{290}$	Bösken *et al.* (in press, a)
C-L3795	Bodrogkeresztúr, Hungary	48°08'50"N, 21°21'48"E	Loess	pIRIR$_{290}$	Bösken *et al.* (in press, b)
C-L3797	Bodrogkeresztúr, Hungary	48°08'50"N, 21°21'48"E	Pedogenetically overprinted loess	pIRIR$_{290}$	Bösken *et al.* (in press, b)
C-L3799	Bodrogkeresztúr, Hungary	48°08'50"N, 21°21'48"E	Loess	pIRIR$_{290}$	Bösken *et al.* (in press, b)

Stokes' Law). All steps were carried out under subdued red light conditions (640 ± 20 nm). Readily prepared fine grains were pipetted onto aluminium or steel discs (~2 mg per aliquot in Bayreuth, ~0.9–1.0 mg in Cologne) for IRSL and pIRIR measurements. Experiments by Kreutzer *et al.* (2014; Table S3) have shown that pIRIR$_{225}$ *a*-values resulting from both 1 mg and 2 mg of sample material per aliquot are identical within uncertainties.

3. INSTRUMENTATION AND DATA ANALYSIS

All measurements were carried out on Risø TL/OSL DA15/DA20 readers, equipped with infrared (875 ± 80 nm) diodes for signal stimulation and an EMI 9235QB15 photomultiplier tube coupled with a Chroma D410/30x band pass filter (410 ± 15 nm) for signal discrimination and detection. Artificial β-irradiation was carried out with a built-in ^{90}Sr/^{90}Y β-source delivering dose rates to fine grains between 0.040 ± 0.002 and 0.133 ± 0.005 Gy s^{-1}. In Bayreuth, α-irradiation was conducted in vacuum (<10^{-2} mbar) using either the built-in ^{241}Am source (0.144 ± 0.007 Gy s^{-1}) of one of the Risø readers or an external six-seater Littlemore ^{241}Am irradiation facility (type 721/B) with a dose rate of 0.021 ± 0.002 Gy s^{-1}. In Cologne, the built-in α-source of a Freiberg Instruments lexsyg research reader was used for that purpose (0.197 ± 0.004 Gy s^{-1}, <1 mbar). Information on the calibration of these α-sources is given in the appendix.

Acquired luminescence data were analysed using the program Analyst (v.4.31.9; Duller, 2015). IRSL and pIRIR$_{290}$ decay curves were measured for 300 s (Bayreuth) or 200 s (Cologne) in this study, and the initial 5 s were integrated to give the signal with which dose response curves were constructed. Instrumental background averaged from the last ~40 s of the decay curve was subtracted from the integrated signal.

4. MULTIPLE ALIQUOT ADDITIVE-DOSE (MAAD) MEASUREMENTS

Previous studies on the appropriateness of using single-aliquot regeneration (SAR) protocols for *a*-value assessment raised concerns on the validity of β-test dose correction of α-induced luminescence signals (Mauz *et al.*, 2006). One way of bypassing this problem is to apply multiple-aliquot additive-dose (MAAD) protocols. In this study, natural aliquots were divided into four dose groups (four aliquots each) and given equally-spaced additive α-doses between 0 and 969 Gy. After measuring the pIRIR$_{290}$ and IRSL$_F$ signals according to the protocol described in **Table 2** (steps 2–4), the fitted dose response curve was extrapolated to the α-dose axis and the so-obtained α-dose related to the β-dose derived from 'regu-

lar' SAR D_e measurements to obtain the *a*-value. We adopted the equal pre-dose normalisation technique (Franklin and Hornyak, 1992) to reduce inter-aliquot scatter using solely α-regeneration doses and an α-test dose of 211 Gy. In the course of this normalisation method, all aliquots received the same cumulative dose and heat treatment prior to test dose irradiation to consider dose-dependent sensitivity changes. To account for the pIRIR$_{290}$ residual, the signal left after 24 h bleaching in a solar simulator (Osram Duluxstar 24 W) was subtracted (**Fig. 1**). In all cases, the laboratory bleaching procedure resulted in IRSL$_F$ and pIRIR$_{290}$ signals close to instrumental background levels. For MAAD investigations, we chose two samples (BT1344, BT1345) with comparably small D_e values with the aim to enable a linear fit to the dose points. The MAAD dose response curve of sample BT1345 is shown in **Fig. 1**; resulting *a*-values are listed in **Table 4**.
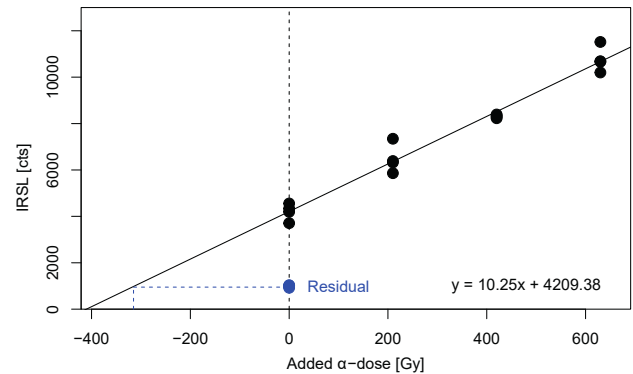

Fig. 1. *Results of MAAD measurements for sample BT1345 (IRSL$_F$ protocol). The corresponding a-value is shown in Table 4.*

Despite the fact that *a*-values derived from MAAD measurements may be regarded as reliable for the above mentioned reasons (no test dose correction necessary and normalisation using α-doses only), they are nevertheless tied to some impracticalities. First, comparatively large amounts of sample material are required (>12 aliquots, in addition to those needed for 'regular' D_e determination). Secondly, data scatter and extrapolation of the dose response curve can cause uncertainties of dose estimates usually larger than those in SAR measurements. The following experiments hence aim at testing whether SAR measurements are a practical alternative to the MAAD approach and which measurement procedures yield the most reliable *a*-values. The pIRIR$_{290}$ protocol following Thiel *et al.* (2011) and the IRSL$_F$ protocol after Faust *et al.* (2015) on which the SAR measurements are based are outlined in **Table 2**.

Table 2. *Measurement protocols employed for a-value determination. Step 1 in the first SAR cycle is carried out using α-irradiation, while all subsequent irradiations refer to β-doses. The pIRIR$_{290}$ protocol follows Thiel et al. (2011), while the IRSL$_F$ protocol was adopted from Faust et al. (2015). Stimulation times for IRSL$_{50}$ and pIRIR$_{290}$ signals were 300 s (Bayreuth) or 200 s (Cologne); an IRSL readout at 325°C for 600 s (Bayreuth) or 200 s (Cologne) intended to fully zero IRSL traps prior to the next regeneration cycle.*

|	pIRIR$_{290}$			IRSL$_F$	
Step	Procedure	Signal	Step	Procedure	Signal
0	Resetting of the natural signal		0	Resetting of the natural signal	
1	Irradiation with dose D_i		1	Irradiation with dose D_i	
2	Preheat (320°C, 60 s)		2	Preheat (270°C, 120 s)	
3	IR stimulation (50°C, 300 s or 200 s)		3	Pause (1200 s)	
4	IR stimulation (290°C, 300 s or 200 s)	L_x	4	IR stimulation (125°C, 300 s)	L_x
5	Irradiation with test dose D_t		5	Irradiation with test dose D_t	
6	Preheat (320°C, 60 s)		6	Preheat (270°C, 120 s)	
7	IR stimulation (50°C, 300 s or 200 s)		7	Pause (1200 s)	
8	IR stimulation (290°C, 300 s or 200 s)	T_x	8	IR stimulation (125°C, 300 s)	T_x
9	IR stimulation (325°C, 600 s or 200 s)		9	Return to step 1	
10	Return to step 1				

5. SINGLE ALIQUOT REGENERATION (SAR) MEASUREMENTS

Considerations on the size of regeneration doses

The determination of the *a*-value relies on comparing luminescence signals generated by α- and β-radiation. Since the α-dose response is linear to much higher doses than the β-dose response, the *a*-value starts to change as soon as the β-dose response shows saturating behaviour (Zimmerman, 1972; Mauz *et al.*, 2006; Kreutzer *et al.*, 2014). It is thus important to avoid doses outside the linear range of the dose response for both α- and β-radiation. Depending on the individual luminescence sensitivity of each sample, we therefore tried to keep administered α- and β-regeneration doses as low as possible (**Table 4**). Due to this restriction and the fact that the intensity of pIRIR signals usually exceeds that of the IRSL$_{50}$ signals for stimulation temperatures >250°C (e.g., Zhang *et al.*, 2015), the latter signal was too dim in most cases to evaluate IRSL$_{50}$ *a*-values accurately.

pIRIR signal resetting prior to α-regeneration

A common SAR procedure to determine the *a*-value includes irradiating a zeroed aliquot with a known α-dose, constructing a dose response curve by a series of β-regeneration cycles and finally dividing the obtained β-D_e by the known α-dose. Kreutzer *et al.* (2014) showed for the pIRIR$_{225}$ emission of polymineral fine grain samples that the mechanism of signal resetting prior to α-irradiation has significant influence on the resulting *a*-value. Without being able to cover the entire set of zeroing mechanisms examined by Kreutzer *et al.* (2014) for all of our samples, we focus here on thermally-assisted IR resetting ('hot bleach') and annealing. While samples at the Bayreuth laboratory received a hot bleach (IR stimulation at 325°C for 600 s, identical to step 9 in **Table 2**), those in the Cologne laboratory were annealed

(480°C for 60 s) for the purpose of signal resetting. Both procedures cause IRSL and pIRIR$_{290}$ signal depletion down to levels indistinguishable from instrumental background. For three samples from the Cologne laboratory (C-L3787, C-L3789, C-L3793) and one from the Bayreuth laboratory (BT1344) both resetting procedures were applied in parallel. Three of these samples gave identical *a*-values for both resetting methods, while one (C-L3789) showed differing results (based on the standard deviation of individual aliquots) (**Fig. 2**; **Table 4**). Observed differences between the resetting procedures are not significant (Welch two sample *t*-test: $t = 0.85$, $df = 8.0$, $p = 0.42$).
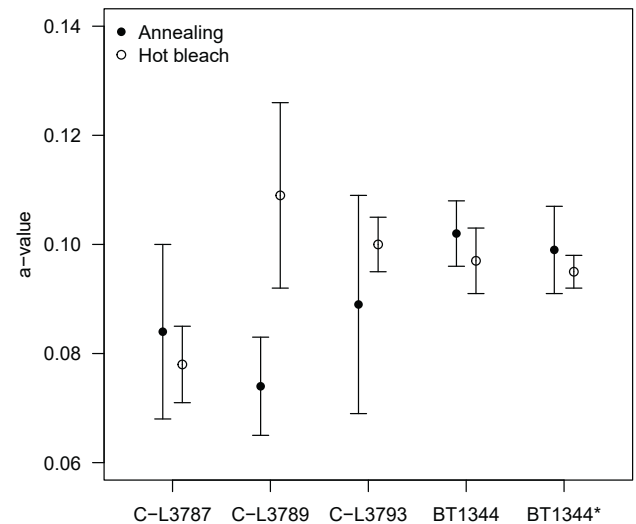
Fig. 2. *Comparison of a-values determined following different luminescence signal resetting modes. Each data point represents 2–4 individual a-value measurements; the error bars show the standard deviation. All measurements were carried out with aliquots of ~1 mg sample material, except for BT1344* (~2 mg sample material per aliquot).*

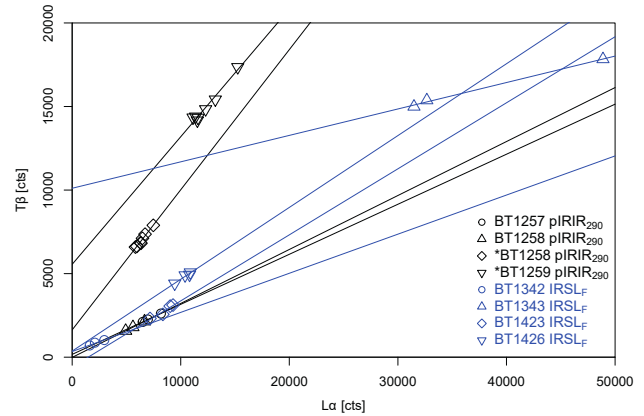## Sensitivity correction of an α-regenerated signal by a β-test dose

One basic assumption of SAR protocols is that the luminescence signal of a test dose measurement monitors the sample's luminescence sensitivity to the preceding regenerative β-dose (e.g., Murray and Wintle, 2000). Whether this assumption holds true for an α-regenerated signal that is monitored by a β-test dose measurement is, however, unclear. Accurate sensitivity correction can be expected if the α-induced luminescence signal (L_α) and the β-test dose signal (T_β) are directly proportional to each other in the course of repeated constant-dose L_α and T_β cycles. In addition, in a plot of T_β vs. L_α the y-axis intercept should be small compared to luminescence intensity (Murray and Mejdahl, 1999). Previous investigations of a silt-sized quartz sample by Mauz *et al.* (2006) showed varying behaviour in the proportionality of L_α and T_β signals, with one aliquot fulfilling these requirements, while the other three failed. Equivalent experiments for silt-sized polymineral samples have not yet been carried out.

We therefore measured repeated $L_\alpha - T_\beta$ cycles for seven polymineral samples (four aliquots each) while applying the two measurement protocols listed in **Table 2**. Natural signals were zeroed prior to α-regeneration by means of a hot bleach and α-doses were chosen according to luminescence signal intensity (BT1257, BT1258, BT1259: 298 Gy; BT1342, BT1343, BT1423, BT1426: 199 Gy); the β-test dose was kept constant at 5 Gy. For practical reasons, the major part of measurements consisted of three cycles of α-irradiation using the Littlemore facility and β-irradiation in a Risø reader. However, to check for potential loss of sample material during repeated transport between irradiation facilities, we conducted reference measurements of seven $L_\alpha - T_\beta$ cycles for samples BT1258 and BT1259 (IRSL$_F$ and pIRIR$_{290}$) using both the built-in α- and β-source of one of the Risø readers, *i.e.* sample transport was not necessary in this case. $L_\alpha - T_\beta$ data were fitted with a linear function. Representative results are shown in **Fig. 3**.

As evident from **Fig. 3**, the major part of studied samples (~70%) revealed direct proportionality between L_α and T_β. There is a substantial offset on the y-axis only for few samples (e.g., BT1343 in **Fig. 3**), rendering the SAR procedure for *a*-value determination inappropriate for these. The relative change of the L_α/T_β ratio after three and seven regeneration cycles for the IRSL$_F$ and pIRIR$_{290}$ protocols is shown in **Table 3** for samples BT1258 and

Fig. 3. *Results of the repeated $L_\alpha - T_\beta$ measurements. Data were fitted with a linear function; pIRIR$_{290}$ results are shown in black, IRSL$_F$ results in blue. The asterisk indicates that seven $L_\alpha - T_\beta$ cycles were measured without removing the samples from the luminescence reader, while the other samples were transferred from the α-irradiation facility to the luminescence reader three times (see main text for further details).*

BT1259. Furthermore, we could not observe any systematic trend with respect to sample provenance and measurement protocol for the fulfilment of the $L_\alpha - T_\beta$ requirement.

Variation of *a*-values among samples and measurement protocols

Since the SAR approach as outlined in the previous sections appears to be appropriate for α-efficiency determination for the majority of polymineral samples, we employed it to determine the *a*-value for the 47 samples listed in **Table 1**. For each sample, up to eleven aliquots were analysed and the arithmetic average calculated, along with the standard deviation (SD, at 1σ confidence level) and the averaged measurement uncertainty $\Delta a = [(\Delta a_1^2 + \Delta a_2^2 + \ldots + \Delta a_n^2)/n]^{0.5}$ (with Δa_n being the uncertainty of an individual aliquot, and *n* the number of aliquots) in order to both depict the scatter of several aliquots of one sample and the uncertainties associated with individual *a*-values derived from a single aliquot. Results are summarised in **Fig. 4** and compiled numerically in **Table 4**.

The *a*-values for the IRSL$_F$ protocol yield an average of 0.081 ± 0.008 (*n* = 24; unweighted average with SD) and 0.074 ± 0.009 (*n* = 24; error-weighted average with SD) (**Table 4** and **Fig. 4**). Excluding the MAAD *a*-value of sample BT1344 (outlier according to Dixon's test with *p* = 0.01; Rorabacher, 1991) produces average pIRIR$_{290}$ *a*-values for samples measured in Bayreuth of 0.085 ± 0.010 (*n* = 18; unweighted average) and 0.083 ± 0.011 (*n* = 18; error-weighted average). Corresponding pIRIR$_{290}$ *a*-values for the measurements conducted in Cologne are 0.101 ± 0.014 (*n* = 22; unweighted average) and 0.095 ± 0.013 (*n* = 22; error-weighted aver-

Table 3. *Relative change of the L_α/T_β ratio after repeated $L_\alpha - T_\beta$ cycles (see main text for further information).*

Sample	BT1258		BT1259	
Protocol	IRSL$_F$	pIRIR$_{290}$	IRSL$_F$	pIRIR$_{290}$
3 cycles	6%	3%	9%	8%
7 cycles	5%	7%	12%	13%

Table 4. *Results of a-value determination. In contrast to Table 1, samples are grouped according to the measurement protocol used for a-value determination. n is the number of measured aliquots per sample. The a-value is derived as the arithmetic mean of individual aliquots of one sample; the averaged measurement uncertainty Δa is calculated using the formula $\Delta a = [(\Delta a_1^2 + \Delta a_1^2 + \ldots + \Delta a_n^2)/n]^{0.5}$; SD is the standard deviation. The low-temperature IRSL readout of sample C-L3789 was carried out both at 50°C and 80°C, as indicated in the first column. Systematic errors relating to α- and β-source calibration are not considered in this compilation.*

Sample code	Protocol	Resetting	α-dose (Gy)	n	a-value	Δa	SD (1σ)
BT1257	pIRIR$_{290}$	Hot bleach	298	4	0.078	0.005	0.005
BT1258	pIRIR$_{290}$	Hot bleach	298	4	0.087	0.005	0.008
BT1259	pIRIR$_{290}$	Hot bleach	298	4	0.083	0.004	0.007
BT1344	pIRIR$_{290}$	Hot bleach	298	4	0.084	0.006	0.009
BT1344	pIRIR$_{290}$ MAAD	Hot bleach	−	−	0.035	0.004	−
BT1345	pIRIR$_{290}$	Hot bleach	633	4	0.102	0.009	0.011
BT1345	pIRIR$_{290}$ MAAD	Hot bleach	−	−	0.075	0.008	−
BT1513	pIRIR$_{290}$	Hot bleach	298	3	0.089	0.005	0.006
BT1515	pIRIR$_{290}$	Hot bleach	298	3	0.077	0.009	0.010
BT1517	pIRIR$_{290}$	Hot bleach	298	3	0.076	0.003	0.003
BT1519	pIRIR$_{290}$	Hot bleach	298	3	0.071	0.005	0.003
BT1525	pIRIR$_{290}$	Hot bleach	298	3	0.094	0.008	0.011
BT1526	pIRIR$_{290}$	Hot bleach	298	3	0.107	0.008	0.004
BT1527	pIRIR$_{290}$	Hot bleach	298	3	0.090	0.010	0.006
BT1528	pIRIR$_{290}$	Hot bleach	298	3	0.075	0.004	0.007
BT1401	pIRIR$_{290}$	Hot bleach	373	2	0.091	0.008	0.008
BT1415	pIRIR$_{290}$	Hot bleach	298	4	0.085	0.004	0.006
BT1416	pIRIR$_{290}$	Hot bleach	298	4	0.083	0.003	0.003
BT1417	pIRIR$_{290}$	Hot bleach	298	4	0.091	0.004	0.007
C-L3704	pIRIR$_{290}$	Annealing	79	2	0.109	0.006	0.009
C-L3707	pIRIR$_{290}$	Annealing	79	2	0.115	0.006	0.008
C-L3778	pIRIR$_{290}$	Annealing	79	3	0.116	0.006	0.010
C-L3780	pIRIR$_{290}$	Annealing	79	2	0.108	0.007	0.015
C-L3784	pIRIR$_{290}$	Annealing	79	3	0.119	0.010	0.016
C-L3786	pIRIR$_{290}$	Annealing	79	2	0.085	0.006	0.009
C-L3787	pIRIR$_{290}$	Hot bleach	197	1	0.078	0.007	−
C-L3787	pIRIR$_{290}$	Annealing	394	6	0.084	0.003	0.016
C-L3788	pIRIR$_{290}$	Annealing	394	6	0.105	0.004	0.010
C-L3789 (50C)	pIRIR$_{290}$	Annealing	79	3	0.103	0.007	0.012
C-L3789 (80C)	pIRIR$_{290}$	Hot bleach	197	3	0.109	0.006	0.017
C-L3789 (80C)	pIRIR$_{290}$	Annealing	296	11	0.074	0.003	0.009
C-L3791	pIRIR$_{290}$	Annealing	394	6	0.084	0.003	0.016
C-L3792	pIRIR$_{290}$	Annealing	394	5	0.091	0.004	0.016
C-L3793	pIRIR$_{290}$	Hot bleach	197	2	0.100	0.004	0.005
C-L3793	pIRIR$_{290}$	Annealing	394	6	0.089	0.003	0.020
C-L3795	pIRIR$_{290}$	Annealing	394	5	0.107	0.004	0.005
C-L3797	pIRIR$_{290}$	Annealing	394	6	0.100	0.004	0.005
C-L3799	pIRIR$_{290}$	Annealing	394	3	0.096	0.004	0.007
C-L4029	pIRIR$_{290}$	Hot bleach	50	5	0.113	0.009	0.010
C-L4030	pIRIR$_{290}$	Hot bleach	50	5	0.120	0.012	0.010
C-L4031	pIRIR$_{290}$	Hot bleach	50	5	0.115	0.010	0.019
BT1337	IRSL$_F$	Hot bleach	199	4	0.077	0.014	0.005
BT1339	IRSL$_F$	Hot bleach	199	4	0.074	0.003	0.003
BT1340	IRSL$_F$	Hot bleach	199	4	0.096	0.009	0.002
BT1341	IRSL$_F$	Hot bleach	199	4	0.099	0.014	0.007
BT1342	IRSL$_F$	Hot bleach	199	4	0.086	0.010	0.008
BT1343	IRSL$_F$	Hot bleach	199	4	0.078	0.003	0.003
BT1344	IRSL$_F$	Hot bleach	199	4	0.091	0.006	0.005
BT1344	IRSL$_F$ MAAD	Hot bleach	−	−	0.079	0.006	−
BT1345	IRSL$_F$	Hot bleach	199	4	0.085	0.007	0.003
BT1345	IRSL$_F$ MAAD	Hot bleach	−	−	0.069	0.004	−

Table 4. *Continuation.*

Sample code	Protocol	Resetting	α-dose (Gy)	*n*	*a*-value	Δ*a*	SD (1σ)
BT1421	IRSL$_F$	Hot bleach	199	4	0.084	0.006	0.006
BT1423	IRSL$_F$	Hot bleach	199	4	0.082	0.006	0.005
BT1424	IRSL$_F$	Hot bleach	199	4	0.087	0.005	0.011
BT1425	IRSL$_F$	Hot bleach	199	4	0.077	0.005	0.005
BT1426	IRSL$_F$	Hot bleach	199	4	0.077	0.003	0.005
BT1432	IRSL$_F$	Hot bleach	199	4	0.080	0.004	0.005
BT1513	IRSL$_F$	Hot bleach	298	3	0.072	0.003	0.001
BT1514	IRSL$_F$	Hot bleach	298	4	0.081	0.005	0.005
BT1515	IRSL$_F$	Hot bleach	298	3	0.078	0.006	0.008
BT1517	IRSL$_F$	Hot bleach	298	3	0.073	0.002	0.002
BT1519	IRSL$_F$	Hot bleach	298	3	0.082	0.005	0.003
BT1525	IRSL$_F$	Hot bleach	298	3	0.085	0.005	0.004
BT1528	IRSL$_F$	Hot bleach	298	3	0.066	0.003	0.001
BT1529	IRSL$_F$	Hot bleach	298	4	0.077	0.004	0.005

age). Although pIRIR$_{290}$ *a*-values from both laboratories overlap within 1σ standard deviation (**Fig. 4**), their difference is significant (Welch two sample *t*-test: $t = 3.96$, $df = 36.6$, $p < 0.01$). Contrarily, *a*-values measured with two different protocols in the Bayreuth laboratory (pIRIR$_{290}$ and IRSL$_F$) derive from one common distribution, *i.e.* the difference of their means is not significant (Welch two sample *t*-test: $t = 1.7$, $df = 30.4$, $p = 0.1$). Finally, the variation between samples from different sample locati ons (e.g. sampled sections) measured with the pIRIR$_{290}$ protocol was investigated (**Fig. 5**). The *F*-test revealed that there are significant differences in the mean *a*-values between the tested sample locations

($F_{9,23} = 4.17$, $p < 0.01$), *i.e.*, the explained variation between mean *a*-values of different locations exceeds the unexplained variation within the *a*-values of one sampled profile. Specifically, we observed significant differences in the *a*-values from Vrsac and Titel (C-L4029–4031 and BT1257–1259; Tukey post-hoc-test: $p = 0.01$), Vrsac and Jable 1, Fuerteventura (C-L4029–4031 and BT1513, BT1515, BT1517; Tukey post-hoc-test: p < 0.01), and Vrsac and Vârghis (C-L4029–4031 and BT1415–1416; Tukey post-hoc-test: $p = 0.04$). There is no significant difference between sample locations for the *a*-values determined with the IRSL$_F$ protocol ($F_{6,14} = 2.56$, $p = 0.07$).
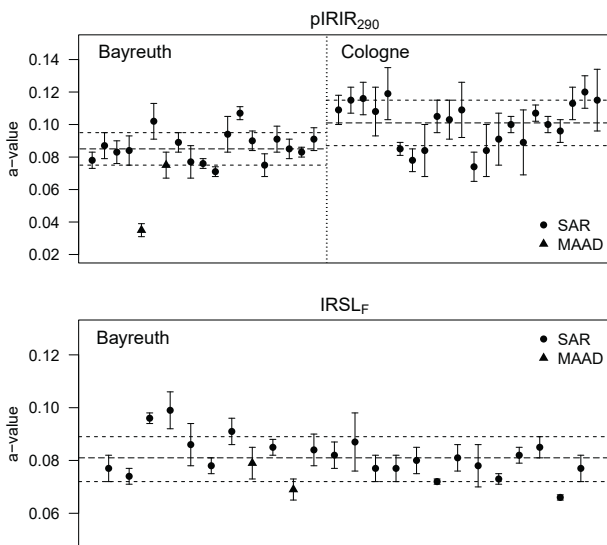
Fig. 4. *Graphical summary of pIRIR$_{290}$ and IRSL$_F$ a-values measured in Bayreuth and Cologne. The dashed lines indicate the unweighted average and its standard deviation (1σ). Data points represent the average of 1–11 aliquots (see Table 4) and are plotted with the corresponding standard deviation (1σ).*
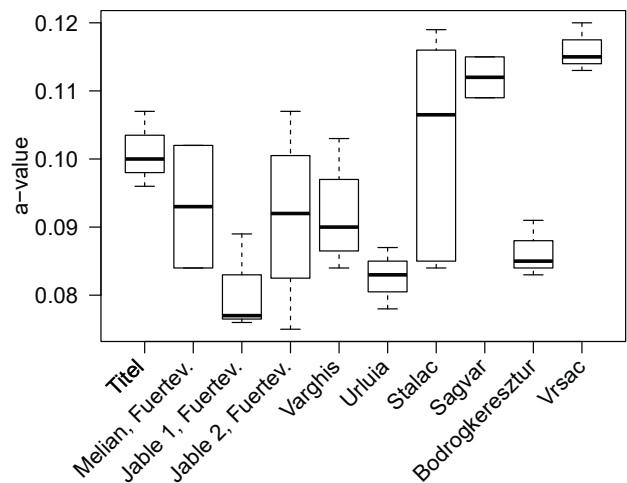
Fig. 5. *Boxplot of pIRIR$_{290}$ a-values grouped according to sampled outcrops. Further sampling information and numerical results are given in Tables 1 and 4.*

Comparative measurements between laboratories

To investigate whether pIRIR$_{290}$ a-values are reproducible on various luminescence readers and with respect to specific laboratory routines, we measured samples prepared in Bayreuth (BT1344) in the Cologne laboratory and vice versa (C-L3778, C-L3788, C-L3791, C-L3707), using the same measurement protocol. However, laboratory-specific resetting mechanisms (Bayreuth: hot bleach; Cologne: annealing) and aliquot size (Bayreuth; ~2 mg; Cologne: ~0.9–1.0 mg) were retained.

Results of these five samples are shown in **Fig. 6**. The pIRIR$_{290}$ a-values obtained are different (by ~20–30%) for the two laboratories, with the values derived in Cologne mostly exceeding those measured in Bayreuth. Nevertheless, these differences are not significant (Welch two sample t-test: $t = 1.82$, $df = 7.7$, $p = 0.11$).

Comparative measurements of sample BT1344 in Cologne using aliquot sizes of ~1.0 and ~2.0 mg yielded identical a-values of 0.097 ± 0.006 and 0.095 ± 0.006, respectively (Welch two sample t-test: $t = 0.53$, $df = 4.8$, $p = 0.62$; see also **Fig. 2**). The pIRIR$_{290}$ a-value hence appears to be largely insensitive to the amount of sample material per aliquot, in accordance to the findings by Kreutzer *et al.* (2014) for the pIRIR$_{225}$ a-value.

In order to further study the potential reasons for differing a-values of the same samples as measured in the two laboratories, we aimed at testing whether there is an offset in actual reading temperature of the two luminescence readers used for the comparative measurements. Therefore, we measured the D_e on a set of fresh aliquots from samples C-L3788 and C-L3791 in Bayreuth, employing a pIRIR protocol as outlined in **Table 2** with three different pIRIR readout temperatures (270, 290, 310°C), while the preheat temperatures were set 30°C lower than the respective stimulation temperatures. Re-
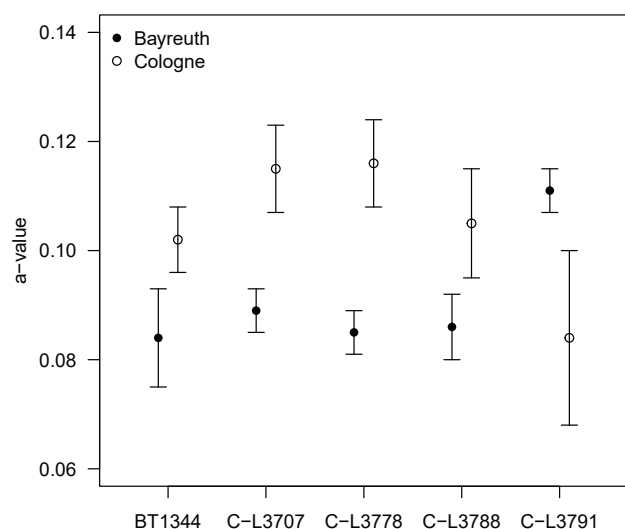
sults are shown in **Fig. 7** and indicate that at least for sample C-L3788 the D_e is rather sensitive to slight variations in preheat and measurement temperature. While for the pIRIR$_{270}$ protocol the D_e amounts to ~245 Gy, it progressively decreases by more than 37% for the pIRIR$_{290}$ (D_e ~ 203 Gy) and the pIRIR$_{310}$ (D_e ~ 154 Gy) protocols. The decrease in D_e with pIRIR measurement temperature is less pronounced for sample C-L3791, with a reduction from ~100 Gy to ~85 Gy. Reconciling these results with the D_e values of the same samples measured in Cologne with the pIRIR$_{290}$ protocol (149 ± 8 Gy and 79 ± 4 Gy for C-L3788 and C-L3791, respectively) suggests an offset of actual measurement temperature of ~20°C in the range 270–310°C.

6. DISCUSSION

Our experiments on the correction of sensitivity changes induced by an α-regeneration dose by means of a β-test dose indicate that for the majority of the investigated samples the SAR protocol (recovery of a known α-dose with β-SAR cycles) is suitable to determine reliable a-values. This procedure is less time- and material-consuming than MAAD protocols, for which sensitivity changes should not have any effect on the results. Comparative a-values derived from SAR and MAAD protocols for four samples (pIRIR$_{290}$ and IRSL$_F$ for two samples each; **Table 4**) are not in agreement within 1σ uncertainties, but are consistent with the overall a-value distribution of the respective IRSL signal and laboratory (see **Fig. 4**; except for the MAAD pIRIR$_{290}$ a-value of sample BT1344, which could be classified as a statistically sig-

Fig. 6. *Results of comparative a-value measurements between the two involved laboratories. Data points represent 2–6 aliquots and are plotted along with the respective standard deviation.*
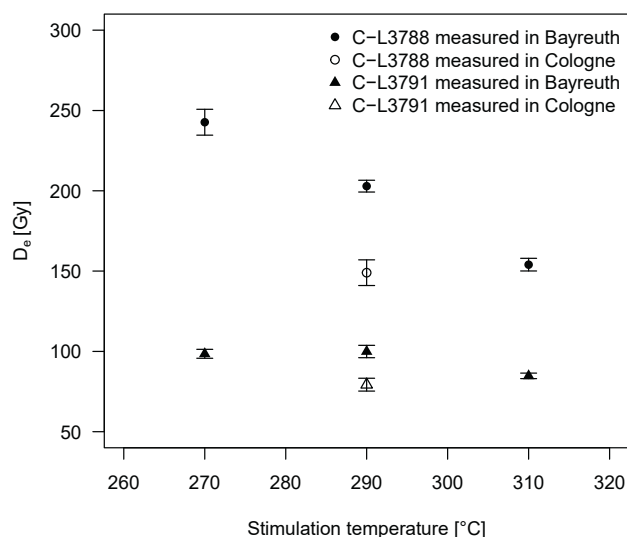
Fig. 7. *Equivalent doses determined with the pIRIR protocol at varying reading temperatures (270, 290, 310°C). Further technical details are given in the main text. A comparative dose estimate derived in the Cologne laboratory using the pIRIR$_{290}$ protocol is indicated with open symbols. Error bars represent the standard deviation of contributing aliquots.*

nificant outlier). Therefore, it can be concluded that SAR protocols are a valid procedure to determine IRSL *a*-values of polymineral silt-sized samples, at least for the majority of samples investigated in this study.

The assessment whether or not there is a common *a*-value for polymineral samples measured with several infrared stimulated luminescence protocols is not straightforward. While *a*-values appear to be consistent within one laboratory environment, there are discrepancies when comparing *a*-values that were obtained using different measurement setups. Although comparative measurements on the same samples in the two laboratories showed differences in *a*-values, these were not significant (but *n* = 5 only). However, considering the entire data set it appears that the *a*-values measured in this study are less dependent on sample origin and lithology, but rather on the measurement equipment and laboratory routines. Since slight variations in experimental conditions may affect the characteristics (anomalous fading, residual signals) of (post-)IRSL signals, measured *a*-values are probably only valid for this respective experimental setup (type of sample carriers, luminescence reader etc.), and D_e and *a*-value measurements on a sample should be carried out with the same setup. Specifically, possible technical reasons for the trend of difference in *a*-values between laboratories could be the calibration of the α- and β-sources, thermal lag or the temperature-calibration of the heating elements in the readers, which seem to be offset, as indicated by the comparative measurements described in the last section. Similar effects were observed in a previous interlaboratory comparison study of the 110°C thermoluminescence peak of quartz (Schmidt *et al.*, 2018). The findings from the pIRIR$_{290}$ D_e comparison of the same samples within two laboratory environments (**Fig. 7**) suggest that the α-source calibration is not the sole cause responsible for the discrepancy in *a*-values between laboratories. For samples with IRSL$_{50}$ signals just high enough to permit determination of rough *a*-value estimates, there is the tendency of higher average IRSL$_{50}$ *a*-values in Cologne (0.086 ± 0.012, *n* = 15) as compared to Bayreuth (0.074 ± 0.009, *n* = 10). Since temperature deviations at 50°C stimulation temperature should be negligible, it appears that systematic shifts in temperature cannot explain the observed *a*-value differences alone. Rather, an interaction of the influencing factors described above seems to cause the observed variation in *a*-values. The aliquot size (~1 mg vs. ~2 mg per aliquot) and the mode of signal resetting, however, do not appear to influence the *a*-value significantly. It is noteworthy that the pIRIR$_{290}$ *a*-values derived after annealing (Cologne) and after hot bleach (Bayreuth) match well with the pIRIR$_{225}$ *a*-values of Kreutzer *et al.* (2014) obtained with comparable resetting mechanisms. Although the comparison of the two resetting mechanisms in our study did not reveal any significant differences in the resulting *a*-values, a consistent pattern with higher *a*-values after annealing emerges. For future research, it

might be advisable to test this with more samples and interlaboratory comparisons.

The slight differences in the pIRIR$_{290}$ measurement protocol (cf. **Table 2**) are unlikely to be the source of *a*-value variations between the two laboratories, because β-regeneration doses and hence signal intensities were usually low. Therefore, pIRIR$_{290}$ signals always reached instrumental background levels at the end of a regenerative measurement and signal carry-over into the test dose cycle as observed by Colarossi *et al.* (2018) appears improbable.

Contrasting the *a*-values obtained from different profiles revealed no provenance-related difference for the samples measured with the IRSL$_F$ protocol. However, these samples were all taken on Fuerteventura in similar geomorphological settings and show comparable geochemical composition. Contrarily, we detected some provenance-related differences between the samples measured with the pIRIR$_{290}$ protocol. It is noteworthy though that these are mainly associated with the only lacustrine archive (Vrsac, Serbia) tested. This might suggest different *a*-values for different types of lithology or sedimentary archives; a statement, however, which needs further investigation. Furthermore, it is possible that slight provenance-related differences in *a*-values are masked by the variation induced through the differences in experimental setup. Therefore, even if there were systematic trends in *a*-values among samples with different lithology, they would not be discernible given the measurement uncertainties. This is supported by the fact that within one laboratory, the *a*-values for most of the samples are statistically the same.

The study of Kreutzer *et al.* (2014) showed for five loess samples from Saxony that the *a*-value appears to rise with increasing sample temperature during measurement (by 0.023 ± 0.012 for IRSL$_{50}$ and pIRIR$_{225}$, respectively, on polymineral fine grains). This trend could not be confirmed with the current data set where the average *a*-values obtained with the IRSL$_F$ and pIRIR$_{290}$ protocols are statistically indistinguishable. Considering *a*-values employed in previous applications of the pIRIR$_{290}$ protocol (e.g., 0.08 ± 0.02 in Thiel *et al.*, 2011; or 0.07 ± 0.02 in Preusser *et al.*, 2014) and the dataset compiled here, it is conceivable that continuing use of literature values could lead to slight, but systematic age overestimation.

Taken previous and the current data together, the *a*-value of IRSL signals from polymineral loess samples appears to range between 0.08 and 0.11, and whenever an individual assessment of *a*-values is not feasible (what is, however, highly encouraged), an increased uncertainty level of 30% could account for the variation in *a*-values caused by differences in measurement equipment and laboratory routines. Nevertheless, to avoid systematic errors in age determination, *a*-values should be measured as accurately as possible for each set of samples and specific measurement setup.

7. CONCLUSION

The analyses conducted in the frame of *a*-value measurements of 47 polymineral silt-samples with two different IRSL measurement protocols (pIRIR$_{290}$ and IRSL$_F$) lead to the following conclusions:

- The SAR protocol appears to be appropriate for determining IRSL *a*-values.
- Within one laboratory environment *a*-values arise from one common statistical population.
- Determining a common and accurate *a*-value, independent of sample mineralogy, provenance and measurement equipment, remains challenging due to an inherent variation between different laboratory environments.
- Measurement equipment seems to exert significant influence on *a*-value results. Therefore, the same luminescence reader should be used for both dose and *a*-value determination.
- For the samples investigated, the *a*-values for the IRSL$_F$ signal average to 0.081 ± 0.008 (unweighted) and range from 0.085 ± 0.010 (Bayreuth laboratory) to 0.101 ± 0.014 (Cologne laboratory) for the pIRIR$_{290}$ signal.

APPENDIX

Alpha-source calibration

The α-source located in the Bayreuth laboratory was cross-calibrated against the six-seater Littlemoore α-source (type 721/B) in the Heidelberg luminescence laboratory by means of a multiple-aliquot regenerative (MAR) dose protocol. Three sets of six aliquots of polymineral fine grains (~4–11 μm) extracted from loess were bleached in a Hönle solar simulator and α-irradiated with doses of 42, 84 and 126 Gy. Another set of six aliquots was bleached in the same manner but α-irradiated with the source in Bayreuth. The resulting integrated IRSL signals were then interpolated onto the dose response curve built using the aliquots irradiated in Heidelberg. The α-dose rate relevant for the source in Bayreuth was obtained from the ratio of determined MAR α-dose and the time of irradiation.

Like the α-source in Bayreuth, the α-source in the lexsyg research reader in the Cologne luminescence laboratory was cross-calibrated against the Heidelberg Littlemoore α-irradiation facility. For the calibration procedure, fine grain (~4–11 μm) quartz was used, from which the natural signal was reset by heating the material at 360°C for ~2 h. The material was divided into two subsets of 24 aliquots each, which received two different α-doses (corresponding to 30 and 60 min irradiation time). These doses were recovered by means of a SAR protocol using α-regeneration and α-test doses. Optimal measurement parameters for this protocol were determined beforehand according to the results of performance tests such as a preheat plateau test. Dose response curves constructed from the signal of the first ~1.3 s of the OSL decay curve (minus a background averaged from the last ~8.3 s) were fitted with a single-saturating exponential function. The results of both subsets were then analysed by using a simple linear regression: In a plot of known α-doses vs. recovered irradiation time the slope of the linear regression was taken as the best estimate for the dose rate of the α-source to be calibrated.

It is important to note that the calibration of an α-source using the *a*-value system is valid for one specific aliquot size only.

REFERENCES

Aitken M, 1985a. Thermoluminescence dating. Academic Press, London.

Aitken M, 1985b. Alpha particle effectiveness: numerical relationship between systems. *Ancient TL* 3: 22–25.

Aitken M and Bowman S, 1975. Thermoluminescence dating: Assessment of alpha particle contribution. *Archaeometry* 17: 132–138.

Biswas R, Williams M, Raj R, Juyal N and Singhvi A, 2013. Methodological studies on luminescence dating of volcanic ashes. *Quaternary Geochronology* 17: 14–25, DOI 10.1016/j.quageo.2013.03.004.

Bösken J, Klasen N, Zeeden C, Obreht I, Marković SB, Hambach U and Lehmkuhl F, 2017. New luminescence-based geochronology framing the last two glacial cycles at the southern limit of European Pleistocene loess in Stalać. *Geochronometria* 44: 150–161, DOI 10.1515/geochr-2015-0062.

Bösken J, Sümegi P, Zeeden C, Klasen N, Gulyás S and Lehmkuhl F, in press (a). Investigating the last glacial Gravettian site 'Ságvár Lyukas Hill' (Hungary) and its paleoenvironmental and geochronological context using a multi-proxy approach. *Palaeogeography, Palaeoclimatology, Palaeoecology*, DOI 10.1016/j.palaeo.2017.08.010.

Bösken J, Obreht I, Zeeden C, Klasen N, Hambach U, Sümegi P and Lehmkuhl F, in press (b). High-resolution proxy data from the MIS3/2 transition recorded in northeastern Hungarian loess. *Quaternary International*, DOI 10.1016/j.quaint.2017.12.008.

Buylaert J-P, Jain M, Murray AS, Thomsen KJ, Thiel C and Sohbati R, 2012. A robust feldspar luminescence dating method for Middle and Late Pleistocene sediments. *Boreas* 41: 435–451, DOI 10.1111/j.1502-3885.2012.00248.x.

Colarossi D, Duller GAT and Roberts H, 2018. Exploring the behaviour of luminescence signals from feldspars: Implications for the single aliquot regenerative dose protocol. *Radiation Measurements* 109: 35–44, DOI 10.1016/j.radmeas.2017.07.005.

Duller GAT, 1992. Luminescence chronology of raised marine terraces, south-west north island, New Zealand. PhD thesis, University of Wales, Abersytwyth.

Duller GAT, 2015. The Analyst software package for luminescence data: overview and recent improvements. *Ancient TL* 33: 35–42.

Faust D, Yanes Y, Willkommen T, Roettig C, Richter D, Richter D, v. Suchodoletz H and Zöller L, 2015. A contribution to the understanding of late Pleistocene dune sand-paleosol-sequences in Fuerteventura (Canary Islands). *Geomorphology* 246: 290–304, DOI 10.1016/j.geomorph.2015.06.023.

Franklin AD and Hornyak WF, 1992. Normalization of inclusion size quartz TL data. *Ancient TL* 10: 1–6.

Jain M and Ankjærgaard C, 2011. Towards a non-fading signal in feldspar: Insight into charge transport and tunnelling from time-resolved optically stimulated luminescence. *Radiation Measurements* 46: 292–309, DOI 10.1016/j.radmeas.2010.12.004.

Kenzler M, Tsukamoto S, Meng S, Thiel C, Frechen M and Hüneke H, 2015. Luminescence dating of Weichselian interstadial sediments from the German Baltic Sea coast. *Quaternary Geochronology* 30: 251–256, DOI 10.1016/j.quageo.2015.05.015.

Kreutzer S, Schmidt C, DeWitt R and Fuchs M, 2014. The *a*-value of polymineral fine grain samples measured with the post-IR IRSL protocol. *Radiation Measurements* 69: 18–29, DOI 10.1016/j.radmeas.2014.04.027.

Li B and Li SH, 2011. Luminescence dating of K-feldspar from sediments: A protocol without anomalous fading correction. *Quaternary Geochronology* 6: 468–479, DOI 10.1016/j.quageo.2011.05.001.

Li B, Roberts RG and Jacobs Z, 2013. On the dose dependency of the bleachable and non-bleachable components of IRSL from K-feldspar: Improved procedures for luminescence dating of Quaternary sediments. *Quaternary Geochronology* 17: 1–13, DOI 10.1016/j.quageo.2013.03.006.

Mauz B, Packman S and Lang A, 2006. The alpha effectiveness in silt-sized quartz: new data obtained by single and multiple aliquot protocols. *Ancient TL* 24: 47–52.

Murray AS and Mejdahl V, 1999. Comparison of regenerative-dose single-aliquot and multiple-aliquot (SARA) protocols using heated quartz from archaeological sites. *Quaternary Science Reviews* 18: 223–229, DOI 10.1016/S0277-3791(98)00055-9.

Murray AS and Wintle AG, 2000. Luminescence dating of quartz using an improved single-aliquot regenerative-dose protocol. *Radiation Measurements* 32: 57–73, DOI 10.1016/S1350-4487(99)00253-X.

Obreht I, Hambach U, Veres D, Zeeden C, Bösken J, Stevens T, Marković SB, Klasen N, Brill D, Burow C and Lehmkuhl F, 2017. Shift of large-scale atmospheric systems over Europe during late MIS 3 and implications for Modern Human dispersal. *Scientific Reports* 7: 5848, DOI 10.1038/s41598-017-06285-x.

Preusser F, Muru M and Rosentau A, 2014. Comparing different post-IR IRSL approaches for the dating of Holocene coastal foredunes from Ruhnu Island, Estonia. *Geochronometria* 41: 342–351, DOI 10.2478/s13386-013-0169-7.

Rees-Jones J, 1995. Optical dating of young sediments using fine-grain quartz. *Ancient TL* 13: 9–14.

Reimann T and Tsukamoto S, 2012. Dating the recent past (500 years) by post-IR IRSL feldspar – Examples from the North Sea and Baltic Sea coast. *Quaternary Geochronology* 10: 180–187, DOI 10.1016/j.quageo.2012.04.011.

Roettig C-B, Kolb T, Wolf D, Baumgart P, Richter C, Schleicher A, Zöller L and Faust D, 2017. Complexity of Quaternary aeolian dynamics (Canary Islands). *Palaeogeography, Palaeoclimatology, Palaeoecology* 472: 146–162, DOI 10.1016/j.palaeo.2017.01.039.

Rorabacher DB, 1991. Statistical treatment for rejection of deviant values: critical values of Dixon's "Q" parameter and related subrange ratios at the 95% confidence level. *Analytical Chemistry* 63: 139–146, DOI 10.1021/ac00002a010.

Schatz A-K, Buylaert J-P, Murray AS, Stevens T and Scholten T, 2012. Establishing a luminescence chronology for a palaeosol-loess profile at Tokaj (Hungary): A comparison of quartz OSL and polymineral IRSL signals. *Quaternary Geochronology* 10: 68–74, DOI 10.1016/j.quageo.2012.02.018.

Schmidt ED, Tsukamoto S, Frechen M and Murray AS, 2014. Elevated temperature IRSL dating of loess sections in the East Eifel region of Germany. *Quaternary International* 334–335: 141–154, DOI 10.1016/j.quaint.2014.03.006.

Schmidt C, Schaarschmidt M, Kolb T, Büchel G, Richter D and Zöller L, 2017. Luminescence dating of Late Pleistocene eruptions in the Eifel Volcanic Field, Germany. *Journal of Quaternary Science* 32: 628–638, DOI 10.1002/jqs.2961.

Schmidt C, Friedrich J, Adamiec G, Chruscinska A, Fasoli M, Kreutzer S, Martini M, Panzeri L, Polymeris GS, Przegietka K, Valla PG, King GE and Sanderson DW, 2018. How reproducible are kinetic parameter constraints of quartz luminescence? An interlaboratory comparison for the 110°C TL peak. *Radiation Measurements* 110: 14–24, DOI 10.1016/j.radmeas.2018.01.002.

Stevens T, Markovic SB, Zech M, Hambach U and Sümegi P, 2011. Dust deposition and climate in the Carpathian Basin over an independently dated last glacial-interglacial cycle. *Quaternary Science Reviews* 30: 662–681, DOI 10.1016/j.quascirev.2010.12.011.

Thiel C, Buylaert J-P, Murray AS, Terhorst B, Hofer I, Tsukamoto S and Frechen M, 2011. Luminescence dating of the Stratzing loess profile (Austria) - Testing the potential of an elevated temperature post-IR IRSL protocol. *Quaternary International* 234: 23–31, DOI 10.1016/j.quaint.2010.05.018.

Thomsen K, Murray AS, Jain M and Boetter-Jensen L, 2008. Laboratory fading rates of various luminescence signals from feldspar-rich sediment extracts. *Radiation Measurements* 43: 1474–1486, DOI 10.1016/j.radmeas.2008.06.002.

Trauerstein M, Lowick SE, Preusser F and Schlunegger F, 2014. Small aliquot and single grain IRSL and post-IR IRSL dating of fluvial and alluvial sediments from the Pativilca valley, Peru. *Quaternary Geochronology* 22: 163–174, DOI 10.1016/j.quageo.2013.12.004.

Vasiliniuc S, Vandenberghe D, Timar-Gabor A, Panaiotu C, Cosma C and van den Haute P, 2012. Testing the potential of elevated temperature post-IR IRSL signals for dating Romanian loess. *Quaternary Geochronology* 10: 75–80, DOI 10.1016/j.quageo.2012.02.014.

Veres D, Cosac M, Schmidt C, Muratoreanu G, Hambach U, Hubay K, Wulf S and Karátson D, 2018. New chronological constraints for Middle Palaeolithic (MIS 6/5-3) cave sequences in Eastern Transylvania, Romania. *Quaternary International* 485: 103–114, DOI 10.1016/j.quaint.2017.07.015.

Wintle AG, 1973. Anomalous fading of thermoluminescence in mineral samples. *Nature* 245: 143–144, DOI 10.1038/245143a0.

Zeeden C, Hambach U, Klasen N, Fischer P, Obreht I, Papadopoulou M, Chu W, Schulte P, Bösken J, Schäbitz F, Gavrilov MB, Veres D, Marković SB, Vött A and Lehmkuhl F, in prep. A Late Quaternary lacustrine record from the south-eastern Carpathian Basin in the context of aeolian sediments.

Zhang J, Tsukamoto S, Nottebaum V, Lehmkuhl F and Frechen M, 2015. D_e plateau and its implications for post-IR IRSL dating of polymineral fine grains. *Quaternary Geochronology* 30: 147–153, DOI 10.1016/j.quageo.2015.02.003.

Zimmerman D, 1972. Relative thermoluminescence effects of alpha and beta radiation. *Radiation Effects* 14: 81–92.